J Mater Sci (2007) 42:3117–3123
DOI 10.1007/s10853-006-0522-9

Thermo-mechanical and microstructural characterisation of sodium-poly(sialate-siloxo) (Na-PSS) geopolymers

Subaer · Arie van Riessen

Received: 5 June 2005 / Accepted: 6 June 2006 /

Abstract The thermo-mechanical and microstructural character of sodium-poly(sialate-siloxo) (Na-PSS) geopolymers synthesised from dehydroxylated kaolinite (metakaolinite) have been investigated. Thermal analysis by means of TG–DTA showed a single endothermic peak at 135–140 °C due to dehydration (water evolution) from the geopolymer framework. Thermal expansion measurements show that geopolymer suffers 2% shrinkage below 250 °C and is then dimensionally stable up to 800 °C. The inclusion of aggregate (α-quartz or granite) was found to reduce the shrinkage by 1% although the presence of the quartz limits the working temperature range of the composite due a to disruptive phase change. Thermal conductivity and compressive strength of Na-PSS geopolymers varied with change in chemical composition of the geopolymer as well as the amount and type of aggregate. Investigation of the microstructure by electron microscopy showed that the ratio of the starting materials influences the homogeneity of the geopolymer microstructure, which in turn leads to differences in thermal conductivity and compressive strength.

Introduction

Over the past two decades, geopolymers manufactured from alkali-activation of silico-aluminate emerged as a new material with a wide variety of potential applications. Davidovits [1, 2] and Rahier et al. [3, 4] proposed the structure of geopolymers as a polymeric Si–O–Al framework (sialate), with SiO_4 and AlO_4 tetrahedra linked alternatively by sharing all the oxygen atoms. The presence of cations such as K^+, Na^+ and Ca^+ in the framework is essential to balance the negative charge of AlO_4.

Geopolymers can be manufactured into three different units of sialate, depending on the atomic ratio of Si:Al; (poly-sialate) M^+ (–Si–O–Al–O–) (PS), poly-sialate siloxo M^+ (–Si–O–Al–O–Si–O–) (PSS) and poly-sialate-disiloxo M^+ (–Si–O–Al–O–Si–O–Si–O–) (PSDS). The M^+ is typically an alkali ion, commonly Na^+ or K^+. By changing the ratio of Si:Al and Na:Al, the resulting materials would have different physical and mechanical properties [1–3, 5]. Polysialate-siloxo for example can be used as a refractory, high performance cement and for immobilisation of toxic waste [2, 6–8].

Since geopolymers are a potential substitute material for ordinary Portland cement (OPC) as well as being suitable for high temperature applications, their thermal properties such as thermal expansion and thermal conductivity is of interest. This paper reports the thermo-mechanical properties of sodium polysialate-siloxo (Na-PSS) geopolymers with and without α-quartz and granite aggregate. Microstructural characterisation of the samples was performed using scanning electron microscopy (SEM) and transmission electron microscopy (TEM).

Experimental

Sodium-poly(sialate-siloxo) geopolymers were synthesised from metakaolinite and activated with an

Subaer · A. van Riessen (✉)
Centre for Materials Research, Department of Imaging & Applied Physics, Curtin University of Technology,
PO Box U 1987, Perth, WA 6845, Australia
e-mail: a.vanriessen@curtin.edu.au

alkaline solution. Metakaolinite was obtained by dehydroxylation of kaolinite at 750 °C for about 6 h. The kaolinite used in this study was paint/filler grade kaolin clay (Kingwhite 65) supplied by Unimin Australia Limited. Technical grade sodium silicate solution (Sigma Chemicals Ltd.) was used as an activator and the soda content was increased by the addition of sodium hydroxide. The chemical compositions of these starting materials are presented in Table 1. Table 2 shows the molar oxide ratios used in the production of the geopolymers. The molar oxide ratio of H_2O:Na_2O was kept constant at 10. At this value the water content of the sodium silicate mixture was adequate to facilitate geopolymerisation without deterioration of the mechanical properties of the geopolymer. Geopolymer samples were made by the addition of metakaolinite powder to the sodium silicate + sodium hydroxide + water mixture followed by mixing until homogeneous. The mixture was then placed into polycarbonate cylindrical moulds (6.0 cm in height and 2.5 cm in diameter). Samples were then cured at 70 °C for 2 h. For some samples, natural sand in the form of α-quartz or crushed granite with different particle size was used as aggregate.

After drying, the samples were sectioned into 1 cm high cylinders for bulk density and apparent porosity measurements, which were determined using Archimede's principle (ASTM Standard C20). Samples for compression tests were 5.0 cm in height and 2.5 cm in diameter. The compression tests were conducted using a Wykeham Farrance 50 ton compression machine with a crosshead velocity of 0.33 mm/min.

Imaging of the geopolymer microstructure was undertaken with a Philips XL30 scanning electron microscopy (SEM) equipped with an Oxford energy dispersive X-ray spectrometer (EDS). Before placing samples in the SEM they were either coated with gold for imaging or carbon for elemental analysis. Higher resolution imaging was done using a JEOL 2011 transmission electron microscope (TEM) equipped with an Oxford EDS. Samples for TEM examination were prepared by using a dimple grinder followed by ion beam milling. Images were obtained using an accelerating voltage of 200 kV.

Table 1 Chemical composition of starting materials

Component (%)	Kaolinite	Sodium silicate
Al_2O_3	37.8	–
SiO_2	46.4	30.1
K_2O	0.21	–
Na_2O	0.01	9.4
CaO	0.08	–
MgO	0.15	–
Fe_2O_3	0.8	–
TiO_2	0.8	–
LOI (1000 °C)	13.8	–
H_2O	–	60.5

In this study, the thermal analysis was performed by means of thermogravimetry and differential thermal analysis (TG–DTA). TG–DTA measurements were performed on a SDT Q600 V3.4 Texas Instrument. In all cases, the heating rate was 10 °C/min measured with Pt/Pt-10%Rh thermocouples. Samples of approximately 10 mg were placed in a platinum crucible and heated up to 900 °C with the reference crucible empty.

A DI-24 Adamel Limohargy dilatometer was used to measure the thermal expansion and shrinkage behaviour of 4 mm diameter cylindrical samples of 25 mm height. The measurements were conducted over the range of 20–900 °C with a heating rate of 2 °C/min.

The thermal conductivity of geopolymers was measured using a transient hot wire method. The hot wire method is most commonly used to measure the thermal conductivity of refractories such as insulating bricks and powder or fibrous materials. Because it is basically a transient radial flow technique, isotropic specimens are required. The sample is cylindrical in shape with a length of 25.0 cm and a radius of 5.0 cm. Current through a 0.25 mm diameter nichrome wire imbedded along the axis of the sample was used as a line heat source. The temperature alongside the line heat source was measured with an imbedded thermocouple and a second thermocouple measured the surface temperature (Fig. 1).

The mathematical principle of the hot wire method is that an infinite line heat source is imbedded in an infinite medium. The time dependent conduction equation in cylindrical coordinates with temperature varying only in the radial direction is given by [9, 10]:

$$\frac{\partial T}{\partial t} = \lambda \frac{1}{r}\frac{\partial}{\partial r}\left(r\frac{\partial T}{\partial r}\right) \tag{1}$$

where λ is the thermal diffusivity of the sample and r is the radial distance from the line source. The solution of Eq. 1 for a medium with a constant initial temperature, T_0, and a heat input q per unit length of line source is:

$$T - T_0 = -\frac{q}{4\pi k} Ei\left(\frac{-r^2}{4\lambda t}\right) \tag{2}$$

where t is the time after the start of heating and k is the thermal conductivity. Details of the function $Ei\left(\frac{-r^2}{4\lambda t}\right)$ can be found in [10]. For $r^2/4\lambda t \ll 1$ Eq. 2 can be expressed as [10];

Table 2 Molar oxide ratios used in the production of geopolymers

Group	SiO_2:Al_2O_3	Na_2O:SiO_2	H_2O:Na_2O
Na:Al = 0.6	2.00	0.30	10
	2.50	0.24	10
	3.00	0.20	10
	3.50	0.17	10
	4.00	0.15	10
Na:Al = 0.8	2.00	0.40	10
	2.50	0.32	10
	3.00	0.27	10
	3.50	0.23	10
	4.00	0.20	10

$$\Delta T = T - T_0 = \frac{q}{4\pi k} \ln\left(\frac{4\lambda t}{r_w^2 C}\right) \tag{3}$$

where r_w = radius of the wire and $C = e^y$ where $y = 0.5772$ (Euler's constant).

Differentiating Eq. 3 with respect to ln t and solving for k yields:

$$k = \frac{q/4\pi}{d\Delta T/d \ln t} \tag{4}$$

In order to obtain the values of thermal conductivity (k) from experimental data, the temperature rise is recorded as a function of ln t and is fitted using a linear least squares regression. If a is the slope then the equation for k is given by:

$$k = \frac{q}{4\pi a}(W\,m^{-1}\,K^{-1}) \tag{5}$$

Results and discussion

Compressive strength

The experimental results show that the strength of geopolymers is time dependent. The maximum strength of the material is reached 7–14 days after processing. The effect of Si:Al on the compressive strength is shown in Fig. 2. A Si:Al ratio of 1.5 (Na:Al = 0.6) was found to produce the highest compressive strength of 86 ± 8 MPa with a bulk density of 1.68 ± 0.09 g cm^{-3}. It is notable that for samples with Na:Al = 1.0, the strength peaks at a Si:Al = 2.0. For the processing procedure adopted the maximum Si:Al that could be achieved was 2.

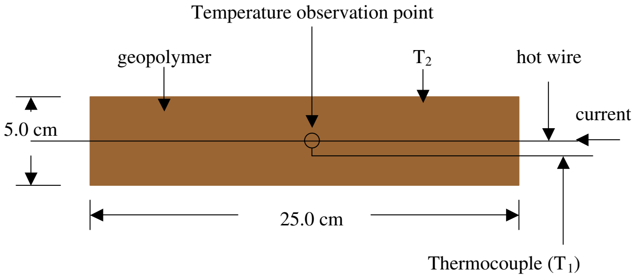

Fig. 1 Schematic diagram of arrangement for measurement of thermal conductivity

Rowles and O'Connor [11] produced Na-PSS geopolymer samples with molar ratios of Si:Al = 2.59, Na:Al = 1.29 by using metakaolinite activated with silica fume plus sodium hydroxide solution. They reported a maximum strength of 64 ± 3 MPa for their geopolymers.

Escalante-Garcia and Sharp [12] measured the compressive strengths of ordinary Portland cement hydrated at various temperatures. They reported that cement cured at 60 °C and aged 7 days has a maximum compressive strength of 42 MPa. The result of this study indicates that the compressive strengths of geopolymers with Si:Al ≥1.5, Na:Al ≥0.6 exceed those obtained for Portland cement.

The trend in the measured compressive strength observed in this study is in good agreement with the results reported by Hos et al. [13]. However, the maximum strength they reported is 5 times higher than that observed in this study. The difference in the strength is probably due to the preparation method as the researchers prepared their samples from melt-quenching a sintered $Al_2O_3 \cdot 2SiO_2$ pellet.

The incorporation of α-quartz or crushed granite aggregate appeared to have negligible effect on the compressive strength of this material as shown in Fig. 3.

Examination of the fracture surface by SEM (Fig. 4) shows evidence of aggregate particles (quartz) being

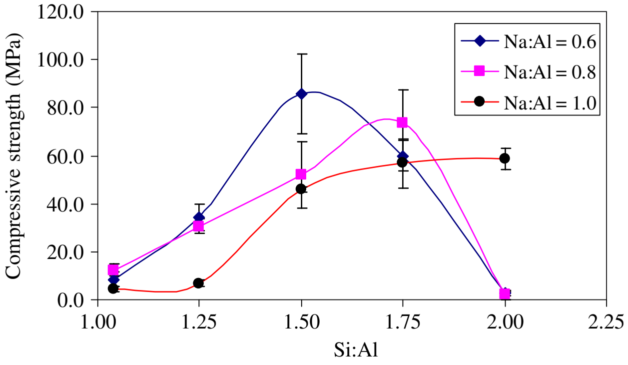

Fig. 2 Compressive strength as a function of Si:Al and Na:Al. Note that these samples were processed without aggregate. Error bars represent two standard deviations

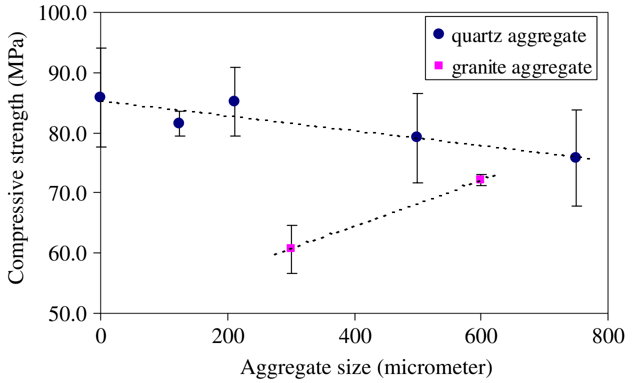

Fig. 3 Compressive strength as a function of aggregate size (Si:Al = 1.5, Na:Al = 0.6). Note that trend lines have only been included to guide the eye. Error bars represent two standard deviations

separated from the geopolymer. No fractured aggregate was observed. Apparently, these aggregates only act as fillers without contributing additional strength. Similar observations were made by Barbosa & MacKenzie [14] who noted a reduction in compressive strength for geopolymers made with six types of aggregates.

Thermal analysis

Figure 5 shows the TG–DTA results from a sample of crushed geopolymer (Si:Al = 1.5, Na:Al = 0.6) from room temperature to 900 °C. The TG curve shows that the sample cured at 70 °C retained about 15% water, of which 8.5% was lost before about 135 °C. The remainder was either bound tightly or less able to diffuse to the surface, and continues to evolve gradually from about 135 up to 500 °C and beyond. The DTA curve is typical for poly(sialate-siloxo) geopolymers showing a single endothermic peak at 135 °C due to dehydration (water evolution). Note that DTA curves for Portland cement normally display two endothermic peaks; the first around 135 °C is attributed the loss of about 10% water and the second endothermic, around 500 °C, is referred to as $Ca(OH)_2$ dissolution [15, 16].

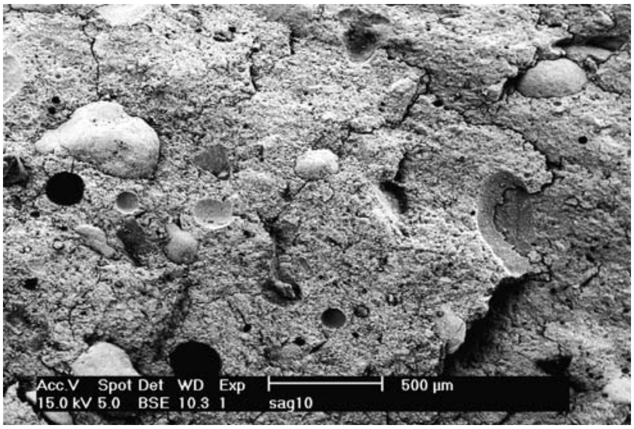

Fig. 4 SEM image of a fractured geopolymer specimen (Si:Al = 1.5; Na:Al = 0.6) containing quartz aggregate. No broken quartz was observed

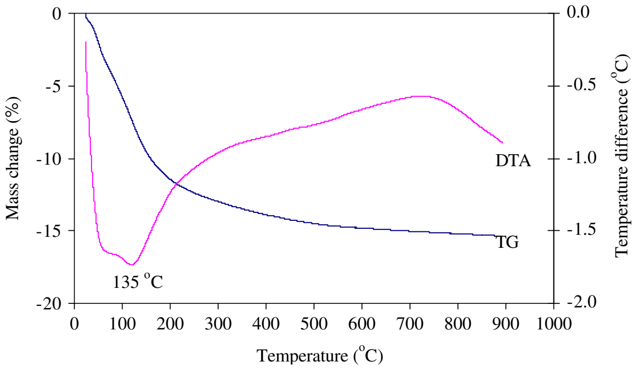

Fig. 5 TG–DTA curves for a geopolymer prepared with Si:Al = 1.5, Na:Al = 0.6

Thermal expansion

Figure 6 shows the dilatometer curves of as prepared geopolymer with Si:Al = 1.50, Na:Al = 0.6 measured from about 23 to 900 °C with a heating rate of 2 °C/min. The curve shows that the water loss (about 15 wt.%) from room temperature up to 250 °C is associated with about 2% shrinkage. Between 250 and 800 °C the geopolymer is essentially dimensionally stable indicating the useful working temperature range of the geopolymer. Further shrinkage from about 800–900 °C occurs due to densification within the sample bulk. At this stage, the sample had shrunk beyond the range of dilatometer LVDT. The shrinkage behaviour

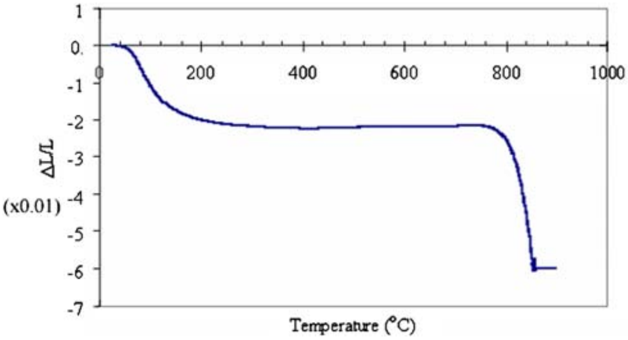

Fig. 6 Dilatometer curve for geopolymer with Si:Al = 1.5, Na:Al = 0.6

of geopolymer reported in this study is in good agreement with the results reported by Barbosa & McKenzie [14].

Neville [17] pointed out that the coefficient of thermal expansion of concrete made from Portland cement is a function of aggregate content and the thermal coefficient of the aggregate itself. Figure 9 shows dilatometer curves for geopolymers containing quartz and granite aggregate. The presence of 20% aggregate was found to significantly reduce the shrinkage to about 1% in the temperature range between 23 and 500 °C. Increasing the content of quartz aggregate to 40 wt% was found to further reduce the shrinkage.

Geopolymers containing quartz aggregate show an abrupt expansion between 500 and 540 °C followed by further shrinkage as the temperature is increased. Raz et al. [18] pointed out that the thermal expansion of quartz is divided into two regions. The first region shows the thermal expansion of quartz increasing rapidly up to the low-high quartz transition (at 574 °C). Above 574 °C the quartz shows negative thermal expansion, it decreases with further increases in temperature. The observed transition temperature is about 40 °C below the literature value of pure quartz 574 °C. This discrepancy arises from the fact that the geopolymer is slightly exothermic (from differential scanning calorimetry measurements) resulting in the interior being hotter than the exterior where the temperature is being measured. Geopolymer containing granite aggregate is dimensionally stable up to 800 °C.

Figure 7 indicates that although the inclusion of quartz has a significant effect in reducing the shrinkage of geopolymers as a function temperature, the useful working temperature range decreases to below 500 °C. It is for this reason that fire-resistant concrete based on Portland cement is never made with quartz aggregate [17].

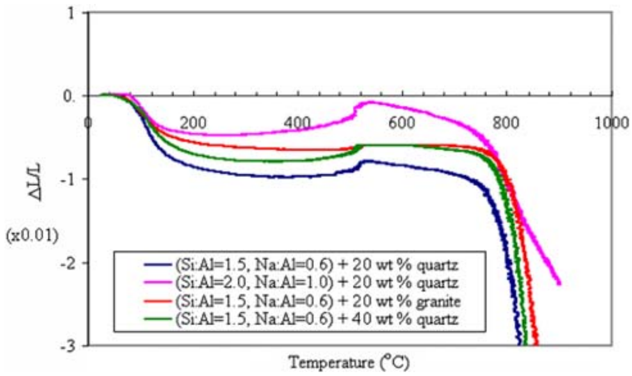

Fig. 7 Dilatometer curves for geopolymers containing quartz and granite aggregate

Thermal conductivity

Table 3 shows the thermal conductivity of geopolymers measured in this study. The difference in thermal conductivity for these samples is believed due to the difference in their bulk density. The addition of 40 wt% of quartz aggregate increased the thermal conductivity by about 40%. This was anticipated since the presence of quartz in the geopolymer structure increased the density resulting in a higher thermal conductivity. The relatively high value of thermal conductivity for geopolymer containing quartz aggregate makes this material suitable as a structural material for buildings and bridges. It is known that a high value of thermal conductivity is desirable as this reduces temperature gradients and lowers thermal stress.

Davidovits [19] reported that the average value of thermal conductivity for geopolymer paste is about 0.7 W m^{-1} K^{-1}. This value, however, can be tailored in accordance to its application. Liefke [20] produced geopolymer foam for thermal insulation having a thermal conductivity of 0.037 W m^{-1} K^{-1} (with a density between 0.1 and 0.8 g cm^{-3}). Neither researcher mentioned the method they used to measure the thermal conductivity of their samples.

The typical value of thermal conductivity of ordinary Portland cement measured by using a laser flash method in conjunction with differential scanning calorimeter (DSC) was 0.53 ± 0.03 W m^{-1} K^{-1} [21]. By using a hot wire method, Demirboga [22] reported that the thermal conductivity of cement paste was (0.76 ± 0.05) W m^{-1} K^{-1} and (1.19 ± 0.05) W m^{-1} K^{-1} for mortar. Santoyo et al. [23] reported that the thermal conductivity of cements for geothermal reservoir application measured by using the hot wire method was between 0.5 and 0.8 W m^{-1} K^{-1}.

The value of thermal conductivity of geopolymer obtained in this study is slightly higher than the thermal conductivity of ordinary Portland cement reported by Xu & Chung [21], but within the range of thermal

Table 3 Thermal conductivity of geopolymers (standards deviations calculated from three measurements are shown in parentheses)

Sample ID	Density (g cm^{-3})	Thermal conductivity (W m^{-1} K^{-1})
(Si:Al = 1.5, Na:Al = 0.6)	1.68 (0.09)	0.65 (0.04)
(Si:Al = 1.5, Na:Al = 0.8)	1.62 (0.05)	0.64 (0.03)
(Si:Al = 2.0, Na:Al = 1.0)	1.43 (0.01)	0.55 (0.03)
(Si:Al = 1.5, Na:Al = 0.6) (40 wt% quartz aggregate)	1.89 (0.02)	0.91(0.07)

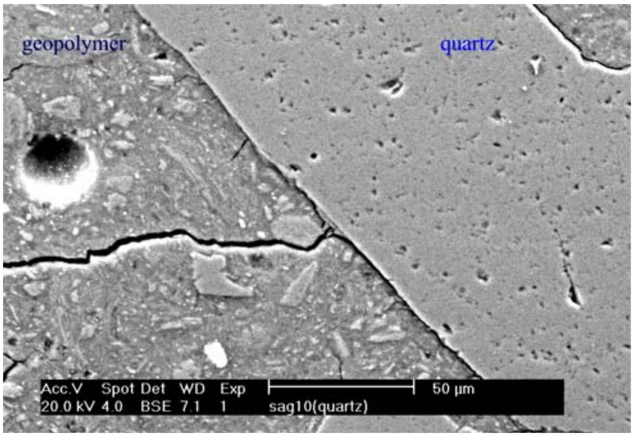

Fig. 8 SEM image of geopolymer (Si:Al = 1.5, Na:Al = 0.6) containing 20 wt% quartz aggregate with a grain size of <500 μm

conductivity reported by Santoyo et al. [23] and Demirboga [22]. The increase of thermal conductivity due to the presence of quartz aggregate in geopolymer is higher than the increase of thermal conductivity observed in Portland cement due to the addition of quartz aggregate.

Microstucture of geopolymers

SEM investigations of the prepared samples revealed a mixture of geopolymer phase, undissolved metakaolinite, and pores in the matrix. SEM-EDS analysis of the geopolymers [24] showed a clear difference in elemental composition and morphology between undissolved metakaolinite and the geopolymer phase. From numerous micrographs it appears that the undissolved metakaolinite also acts like aggregate by deflecting and pinning cracks once they have been initiated.

Figure 8 shows an SEM image of geopolymer (Si:Al = 1.5, Na:Al = 0.6) containing 20 wt% quartz aggregate with a grain size of <500 μm. The image shows a crack coming in from the left and being deflected by a quartz grain.

TEM examination was performed for further microstructural characterisation of the samples. Figure 9 shows a representative TEM image of a geopolymer sample with Si:Al = 1.5, Na:Al = 0.6. The image reveals the original morphology of metakaolinite (mk) bonded to the geopolymer matrix similar to those observed by SEM. The boundary between the undissolved metakaolinite and the matrix is continuous indicating an intimate and strong bond between the two constituents. Some areas of the specimen appear brighter than others indicating a non-uniform thickness of the specimen. Selected area electron diffraction (SAED) from the circled area reveals some degree of ordering has been retained in the metakaolinite (Fig. 10). This indicates that metakaolinite not only maintains its original morphology but may also retain some degree of crystal ordering. The diffraction pattern, however, does not permit determination of the d-spacings to be made with confidence.

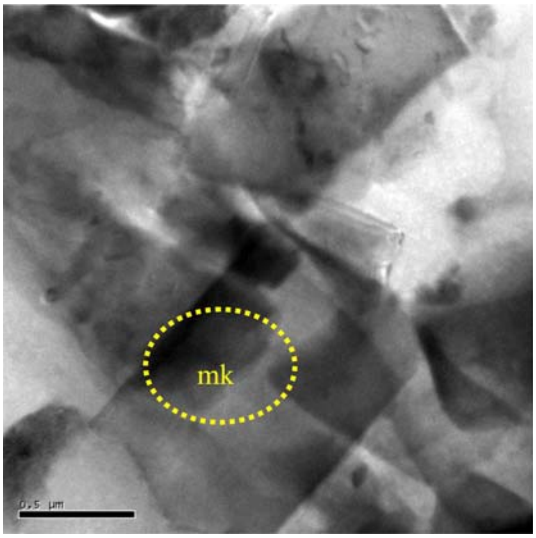

Fig. 9 TEM image of geopolymer sample with Si:Al = 1.5, Na:Al = 0.6. SAED and EDS X-ray analysis was performed in the circled area

The presence of undissolved metakaolinite in the geopolymer structure influences the mechanical and thermal properties of the material mainly through density variations. Microstructural investigation reveals that samples with Si:Al = 2.0, Na:Al = 1.0 contain significantly less undissolved metakaolinite compared to sample with Si:Al = 1.5, Na:Al = 0.6. The

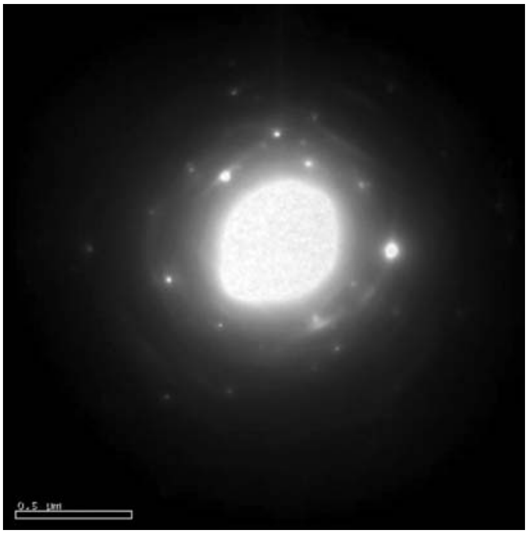

Fig. 10 SAED from the circled area of Fig. 9 showing some degree of retained crystallinity of the grain

strength of these materials is also different as shown in Fig. 2. Table 3 shows that the density as well as thermal conductivity of samples with Si:Al = 2.0, Na:Al = 1.0 are lower than that of samples with Si:Al = 1.5, Na:Al = 0.6.

Conclusion

Sodium poly(sialate-siloxo) (Na-PSS) geopolymers have been produced with excellent thermo-mechanical properties. The compressive strengths of geopolymers was found to depend on the Si:Al and Na:Al ratios and are comparable or better than the strengths of conventional ordinary Portland cement. The loss of water from geopolymer at temperatures below 250 °C caused about 2% shrinkage. Between 250 and 800 °C geopolymer is essentially dimensionally stable. The presence of aggregate (quartz or granite) reduced the shrinkage of geopolymer to 1%. The sudden expansion of quartz at around 574 °C limits the useful working temperature range of geopolymers containing this aggregate. The thermal conductivity of these geopolymers is also similar to those of Portland cement. Microstructural characterisation showed that the samples appear to be a mixture of undissolved metakaolinite particles and geopolymer phase resulting in regions that have mismatched physical properties. Geopolymers with a composition of Si:Al = 2.0, Na:Al = 1.0 are more homogeneous than geopolymers with Si:Al = 1.5, Na:Al = 0.6.

References

1. Davidovits J (1991) J Therm Anal 37:1633
2. Davidovits J (1994) Alkaline cements and concretes. Kiev State Technical University, Ukraine, p 131
3. Rahier H, Van Melle B, Biesemans M, Wastiels J, Wu X (1996) J Mater Sci 31:71
4. Rahier H, Simons W, Van Melle B, Biesemans M (1997) J Mater Sci 32:2237
5. Barbosa VFF, MacKenzie KJD, Thaumaturgo C (2000) Int J Inorg Mater 2:309
6. Lyon RE, Balaguru PN, Foden A, Sorathia U, Davidovits J, Davidovics M (1997) Fire Mater 21:67
7. Van Jaarsveld JGS, Van Deventer JSJ, Lorenzen L (1997) Mine Eng 10(7):659
8. Phair JW, Smith JD, van Deventer JSJ (2003) Mater Lett 4525:1
9. Parrott JE, Stuckes AD (1975) Thermal conductivity of solids. Pion Limited, London
10. Glatzmaier GC, Ramirez WF (1988) Chem Eng Sci 43(12):3157
11. Rowles M, O'Connor BH (2003) J Mater Chem 13(13):1
12. Escalante-Garcia JI, Sharp JH (2001) Cement Concrete Res 31:695
13. Hos JP, McCormick PG, Byrne LT (2002) J Mater Sci 37:2311
14. Barbosa VFF, MacKenzie KJD (2003) Mater Res Bull 38:319
15. Silva FJ, Mathias AF, Thaumaturgo C (1999) Proceedings of Geopolymere '99. Saint-Quentine, France, p 97
16. Vedalakshmi R, Raj AS, Srinivasan S, Babu KG (2003) Thermochim Acta 407(1–2):49
17. Neville AM (2000) Properties of concrete. Prentice Hall, Harlow, p 378
18. Raz U, Girsperger S, Thomson AB, A. B. [available online], http://e-collection.ethbib.ethz.ch/cgi-bin/, 2004 [12 May 2004]
19. Davidovits J [online], http://www.geopolymer.org [21 July 2001]
20. Liefke E (1999) Proceedings of Geopolymere '99. Saint-Quentine, France, p 189
21. Xu Y, Chung DDL (2000) Cement Concrete Res 30:59
22. Demiborga R (2003) Energy Build 35:435
23. Santoyo E, Garcia A, Morales JM, Conteras E, Espinosa-Paredes G (2001) Appl Therm Eng 21:1799
24. Subaer, van Riessen A, O'Connor BH, Buckley CE (2002) J Austr Ceram Soc 38(1):83